INFLUENCE OF ALLOYING ELEMENTS ON MICROSTRUCTURE OF Fe-Cr-Al ALLOY

Adrian Emanuel ONICI [1], Alexandra Mihaela TUDOR[2], Ionelia VOICULESCU[3], Radu STEFANOIU[4], Victor GEANTA[*5]

The paper presents some experimental alloys from the Fe-Cr-Al class alloyed with Zr and Y, that have been obtained using a VAR equipment MRF ABJ 900. The samples were subjected to laser irradiation and severe test conditions, i.e. long-term maintenance in a molten lead environment (6 months), and then they were exposed to irradiation in an intense field of gamma radiation. After being kept in molten lead at 500°C, the samples were extracted, cleaned, then cross-sections were analysed by scanning electron microscopy to evaluate the chemical micro-compositions of the oxide crusts formed on their surface.

Keywords: Alloying, Fe-Cr-Al alloy, microstructure, laser irradiation, chemical composition

1. Introduction

The properties of metallic materials for nuclear power plants are in line with the requirements of new types of nuclear reactors, such as the 4R generation, which cannot operate with standard materials used in previous condition. The intense degradation processes generated by modern working environments (molten lead, molten salts) additional requirements have been imposed for the new families of alloys intended for the manufacture of the 4R generation nuclear reactor vessel, which must have both increased mechanical and corrosion resistance

[1] Assistant, PhD. Eng., Dept. of Engineering and Management of Metallic Materials Obtaining, Faculty of Materials Science and Engineering, National University of Science and Technology POLITEHNICA Bucharest, Romania, e-mail onici.adrian@yahoo.ro

[2] PhD. Eng., Dept. of Quality Engineering and Industrial Technology, National University of Science and Technology POLITEHNICA Bucharest, Faculty of Robotics and Industrial Engineering, Romania, e-mail t.alexandramihaela@yahoo.com

[3] Prof., Dept. of Quality Engineering and Industrial Technology, National University of Science and Technology POLITEHNICA Bucharest, Faculty of Robotics and Industrial Engineering, Romania, e-mail ionelia.voiculescu@upb.ro

[4] Prof.., Dept. of Engineering and Management of Metallic Materials Obtaining, Faculty of Materials Science and Engineering, National University of Science and Technology POLITEHNICA Bucharest, Romania, e-mail radustefanoiu@yahoo.com

[5*] Prof., Dept. of Engineering and Management of Metallic Materials Obtaining, Faculty of Materials Science and Engineering, National University of Science and Technology POLITEHNICA Bucharest, Romania, corresponding author, e-mail victorgeanta@yahoo.com

characteristics, as well as microstructural stability in intense gamma radiation fields [1-2].

Since the operating conditions of generation 4R reactors are in the usual temperature range of 300-1000ºC, the requirements regarding the structural stability of the new materials used are much more severe [3]. Metallic materials used in oxidizing environments and high temperatures can form a protective oxide layer that protects them from the corrosive and erosive actions. Chromium is an alloying element often added to ferritic steels that work at temperatures up to 900°C. But the chromium dioxide that forms on the surface of chromium alloys does not provide sufficient protection against oxidation in extended oxidizing atmospheres at high temperatures. This is mainly due to the formation of cracks in the oxide layer, caused by thermal stress or due formation of volatile CrO_3[4,5]. The addition of small amounts (< 1% wt.) of reactive elements or rare earths leads to an increase in the oxidation resistance of chromium oxide and an increase in adhesion to the metal substrate [6-8].

Fe-Cr-Al alloys are ferritic stainless steels with a high content of aluminum and microalloying elements, and are designed for use at temperatures up to 1400°C. They exhibit remarkable electrothermal properties, such as high resistance, low temperature coefficient, long life at high temperatures, as well as high oxidation resistance performance [9-11]. In this regard, special grades of steel have been designed for the manufacture of the metallic structure of nuclear reactors, which have adequate behaviour in high temperature conditions (600 – 800ºC) and in molten aggressive oxidative environments (Pb, Sn) [12].

By adding small amounts of yttrium (Y), the adhesion and stability of the oxide crust can be improved, and the addition of niobium (Nb) allows precipitation hardening and increased corrosion resistance of Fe-Cr-Al alloys [10]. Alloying with Cu causes the formation of individual FCC solid solutions in the cast Fe-Cr-Al alloy and alloying with Ti promotes the formation of B2-Ni (Al, Ti) and BCC phases in the FCC matrix [8,13]. Zirconium, titanium and rare earths are added to steel to stabilize heat resistance. The creep elongation under load at temperatures above 900°C is considerably reduced and the high temperature resistance is increased. The oxide layer formed improves corrosion resistance, in case of stresses during continuous and/or cyclic heat treatments. Consequently, for applications in oxidizing environments, at temperatures ranging from 900 to 1300 ºC, alloys containing aluminum form a complex oxide layer containing alpha alumina [11-14]. From a thermodynamic point of view, alumina is more stable than chromium dioxide and has a higher melting point. The transport of reactants through alumina is slower compared to that through chromium dioxide. In this context, the presence of aluminum in steels and other alloys containing chromium and working at high temperatures is recommended [15]. Fe-20Cr-5Al alloy are characterized by excellent values of mechanical tensile strength and corrosion resistance at high

operating temperatures, which can be used for the manufacture of the reactor vessel in power plants nuclear generation 4G. These alloys have superior resistance to oxidation at high temperatures compared to ferritic stainless steels. Dense and compact oxide films (of the Cr2O3, Al2O3 or Fe2O3 type) can form on their surface if they are operated at high temperatures, which have the role of blocking the penetration of oxygen into the metal matrix [16].

Recently, research efforts have been focused on creating protective layers on the surface of metals, by cladding with ceramic materials (alumina) [17-19]. During operation in variable temperature regime, due to the difference in thermal expansion coefficients between the metallic matrix and oxide, the ceramic layer can crack or exfoliate, no longer being an effective barrier against the corrosive or erosive effects of the metallic coolant that can provide optimal protection of the installation [20-23].

The paper presents results obtained by adding some microalloying elements to the Fe-Cr-Al alloy, with the aim of improving the corrosion resistance and thermal stability of the oxide layers formed on their surface. The design concept of Fe-Cr-Al alloys doped with yttrium and/or zirconium is presented, after exposure them in harsh environments, such as liquid heavy lead, high temperatures (600ºC) and intense gamma radiation (Co^{-60}), which are specific operating conditions in 4th generation nuclear power plants. Microstructural aspects of the oxide layers formed on the surface of the Fe16Cr8Al alloy microalloyed with Y and Zr were highlighted by SEM analysis and the measurement of the chemical composition in different areas. To improve the aspect, properties and chemical stability of the oxide layers present on the alloy surfaces, laser remelting was performed. The complex oxide layer, containing oxides of Al, Cr, Zr, Y, was funded to be compact and adherent, having different thickness. Prolonged exposure to molten lead caused its diffusion along the grain boundaries in the metallic matrix, as well as the appearance and accumulation of a network of voids.

2. Materials and Methods

2.1. Materials

The design of the chemical compositions of Fe-Cr-Al alloys microalloyed with yttrium and zirconium was performed based on the specific influences of these elements on the properties of alloys, as follows:

- Al content in the alloy was set in the range of 4 to 10wt%, because its ability to form a finely textured and uniform oxide surface, necessary to protect Fe-Cr-Al alloys. For more than 8wt.% Al, there is a drastic reduction in the texturing ability of the aluminum oxide surface, resulting in bundles of alumina fibres, and for lower than 4wt.% Al, adequate oxidation resistance cannot be obtained [9].

- Cr content in the alloy had values in the range of 12 to 18wt.%, to provide a good oxidation resistance and to avoid the tendency of Cr to form the sigma phase (for more than 23wt.%) [13].
- The addition of oxygen-high affinity elements (yttrium, zirconium) leads to the formation of extremely stable oxides on the surface of Fe-Cr-Al alloys, with very high adhesion to the substrate [10, 20].

In the paper, the elements yttrium and zirconium were individually added to experimental Fe-Cr-Al alloys in different concentrations, as follows: Y (1wt.%) and Zr (2.5wt.%). These concentrations were chosen based on the authors' own experimental research [6, 7, 23] and results from the specialized literature [10, 20]. The carbon and nitrogen content of the alloy has been kept to a minimum to avoid the formation of chromium carbides and nitrides, which reduce the local chromium concentration and diminish the ability to restore the protective oxide layer. Therefore, limits of 0.03wt.% C and 0.02wt. N were imposed. Limiting the nitrogen content was achieved by using a vacuum arc melting equipment that working with a minimum vacuum level of 10^{-3} mbar. The limitation of the carbon content was achieved by using as a matrix an ARMCO type raw material (registered trademark MK3) having the chemical composition (wt.%) of 0.02C; 0.04Si; 0.21Mn; 0.02S; 0.015P; 0.2Ni; 0.15Cr; 0.07Mo; 0.14Cu; 0.12Al and the iron content of the alloys resulted from the balance of the recipe elements. The other elements added into the charge were metallic chromium (minimum purity of 99wt.% Cr), electrolytic aluminium (purity of 99.5wt.% Al), and high purity elements like Y and Zr (purity of 99.5 wt.%).

2.2. Methods

The samples were designed and manufactured using a MRF ABJ 900 equipment (fig. 1), in the ERAMET laboratory, at Faculty of Material Science and Engineering from *Politehnica* University of Bucharest. To obtain the alloys, advanced purity raw materials were used, in granular form, which were placed in a copper melting mold, forcedly cooled with water. The melting was carried out with an electric arc in a protective argon environment. After melting, the ingots were twisted and re-melted 5 times, to obtain good homogeneity. The generated laser beam is in the near infrared region and has 975 nm wavelength and 56 mm*mrad maximum divergence. A six axes CLOOS robot was employed for the manipulation of the laser processing head (YW50 Precitec). A minimum tilt angle of 4˚ of the processing head was used to protect the laser optical system.

Fig. 1. MRF ABJ 900 VAR equipment and detail on melting chamber, ERAMET laboratory, Politehnica University of Bucharest, Romania.

The protection of melted bath was ensured by Argon gas coaxially provided within the laser beam, at a flow rate of 14 l/min (Fig. 2b). The laser processing parameters have been laser power of 680W, travel speed of 70cm/min, laser spot diameter of 1.3 mm, working distance of 18 mm. To avoid the cracks appearance on the laser processed surfaces, the samples were preheated at 320 ^{o}C for 30 minutes.

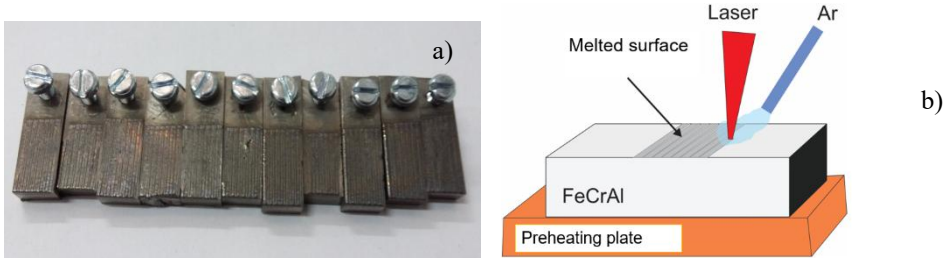

Fig. 2. Laser processed samples prepared for lead immersion (a), and the laser processing schematic (remelting strategy) (b) [17].

Subsequently the samples were continuously kept immersed in melted lead baths at 500 ˚C for 6 months (Fig. 3).

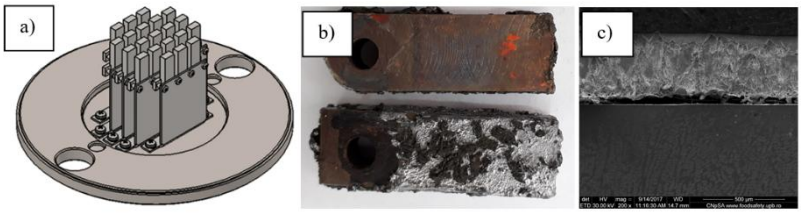

Fig. 3. Schematic of immersion device (a), samples after immersion 6 months in the molten lead bath (b), and SEM cross-section aspect of the lead-rich layer (c).

Then, the samples were exposed to an intense gamma radiation field produced by a Co^{-60} source, dose rate of 310 Gy/h (Fig. 4), with the total dose of 0.3 MGy), for 14 days. The dose rate due to gamma radiation emitted by the two Co^{-60} sources throughout the irradiation period was 288 Gy/h, and the total absorbed dose, depending on the number of days of exposure, was 96.8 kGy (approximately 0.1 MGy) [24]. Irradiation was performed in a solidified lead medium, with d = 234.2 Gy/h, total absorbed dose, D of 5.62 kGy/24 h, and the relative measurement uncertainty (standard deviation) was 3.30%. The irradiation in air was performed with a dose rate d of 410.1 Gy/h, the total absorbed dose D was 29.527 kGy/72 h, and the relative measurement uncertainty (standard deviation) was 3.0% [25-28]. The irradiated samples were measured with the help of a surface GEN-3 Contaminometer device (Ionic Contamination system, Stannol GmbH & Co. KG, Germany), to check the degree of radioactive contamination, before being sent for microstructure analysis.

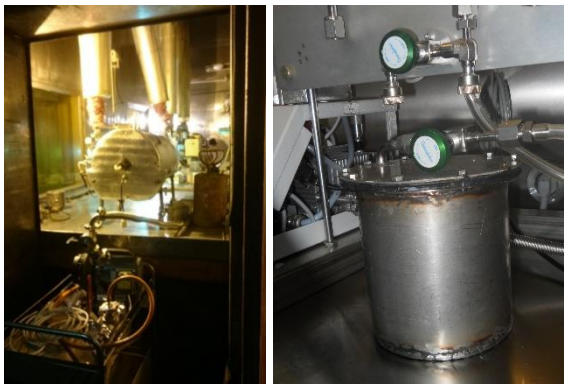

Fig. 4 Irradiation equipment - Gamma 5000 chamber containing a set of Co^{-60} sources distributed circularly with an activity of 8000 Ci [18].

Then, the samples were subjected to optical examinations and microstructural analyses, conducted using a scanning electron microscope FEI QUANTA INSPECT F 50 equipped with electron gun field emission type EGF and a resolution of 1.2 nm, and X-ray spectrometer energy dispersive (EDS) with resolution of 133 eV at MnK. Microhardness was measured with a Shimadzu HMV 2TE apparatus (Tokyo, Japan), using an indentation force of 1.9614 N and a pressing time of 10 seconds. 10 determinations were performed for each area of the sample (from edge to center).

3. Results and Discussion

3.1. Microstructure

The samples were subjected to the metallographic preparation procedure (precise cutting to dimensions of 10x6x4mm, embedding in phenolic resin at 175°C,

polishing with abrasive paper with progressive grits of 600, 800, 1000, 1200, 2500, polishing with abrasive solutions with grit of 1, 0.7 and 0.25 μm). Then, the microstructure was examined after the samples were electrochemically etched with a 10% oxalic acid solution for 10 seconds. The microstructure of the samples was analysed before and after laser remelting (Fig. 5).

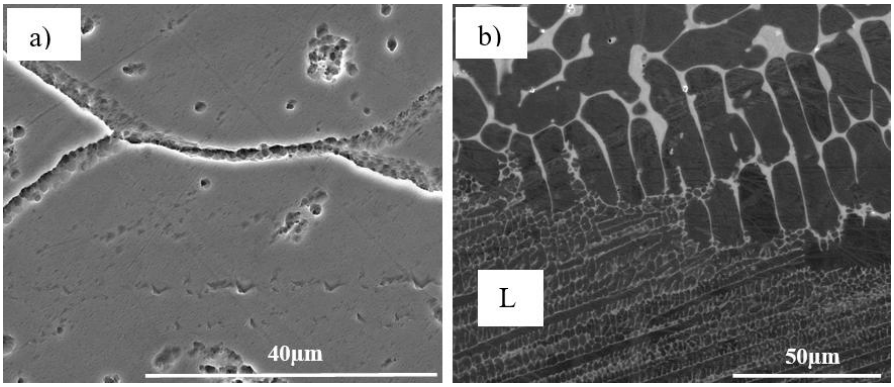

Fig. 5. SEM images of FeCrAl microstructure in as-cast (a) and laser remelting zone "L" (b).

In the as-cast state, the alloys exhibited a dendritic ferrite microstructure with interdendritic precipitations of intermetallic phases containing micro-alloying elements (Fig. 5a). Through laser irradiation, grain finishing and dissolution of some intermetallic compounds were achieved (Fig. 5b).

The microstructure details of the Fe16Cr8Al2.5Zr1.25Y alloy in the as-cast state is shown in Fig. 6. To evaluate the distribution of alloying elements within the metal matrix, EDS chemical composition analyses were performed on micro-zones located in dendrites and in the interdendritic space.

EDS analyses revealed the segregation of the microalloying elements like Y and Zr, mainly in the eutectic phase (Fig. 6c). The chemical composition of the micro-zones from the Fig. 6 are (wt.%): Zone 1 – Zr-rich compound (5.31Al, 4.73Y, 28.68Zr, 12.33Cr, 48.95Fe); Zone 2 - eutectic (7.94Al, 7.26Y, 10.85Zr, 11.15Cr, 62.80Fe); Zone 3 – eutectic (8.64Al, 3.54Y, 9.93Zr, 12.25Cr, 65.64Fe); Zone 4 – metallic matrix (7.7Al, 18.01Cr, 74.29Fe).

The chemical composition of the eutectic is richer in micro-alloying elements compared to the alloy recipe, where concentrations of maximum 3wt.% for Zr and maximum 1wt.% for Y are provided. It is found that these chemical elements tend to segregate in the interdendritic areas, high concentrations being observed in the vicinity of the surfaces of the cast samples.

To evaluate the diffusion distances of lead and oxygen in the alloy surface, chemical composition analyses were performed over a distance perpendicular to the surface exposed to the working environment (Fig. 7). A decrease in the oxygen concentration from 15.75 at the surface level to 1.2 (point 13 in Fig. 7, located at

5.88 µm from the sample surface), respectively of the Pb concentration from 5.46 to 1.70, was observed.

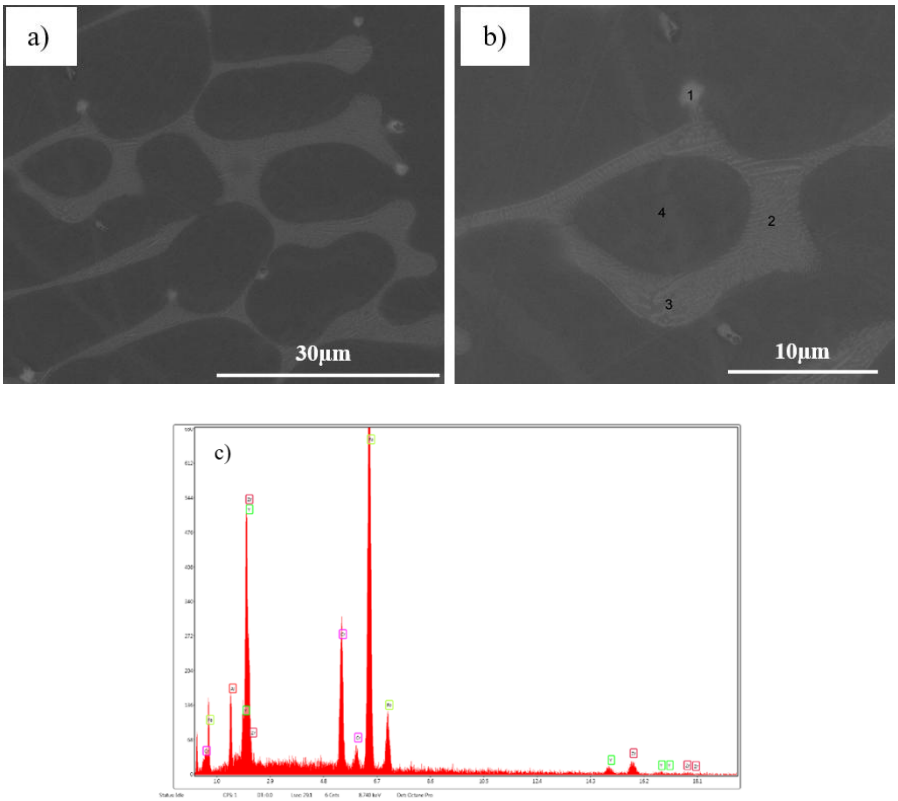

Fig. 6. SEM and EDS analyse of the Fe16Cr8Al2.5Zr1.25Y alloy. a) dendritic metallic matrix; b) detail of the surface layer containing (Zr and Y) rich phases; c) chemical elements spectrum for the micro-zones selected in Fig. 6b.

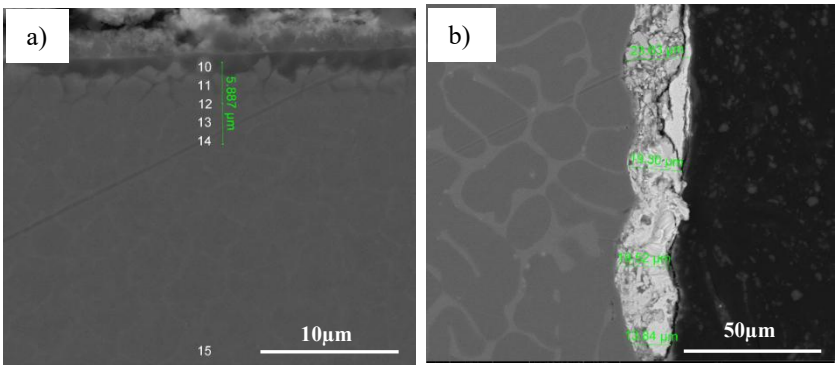

Fig. 7. Distribution of points where the chemical composition was determined, located in the vicinity of the surface exposed to the working environment (a) and the appearance of the adherent lead layer on the sample surface (b) [23].

The Zr concentration in the analysed area recorded the maximum value of 5.71wt.% at measurement point 14. In the other areas, the concentration ranged between the minimum value of 2.81wt.% (point 11) and the maximum value of 5.55wt.% (point 12). These differences are explained by higher values in the eutectic areas, respectively lower values in the dendritic metal matrix. Element Y presented similar chemical composition variations, with values ranging from a minimum of 1.27wt.% in point 11 to a maximum of 4.93wt.% in point 15. The average thickness of the adherent Pb layer was about 15 μm.

Chemical composition measurements performed on the adherent Pb layer revealed significant values of Zr and Y concentration. Thus, the highest Zr concentration was 7.3wt.% and that of Y was 4.27wt.%. These values highlight the fact that the oxide layer recorded higher concentrations of microalloying elements compared to the metallic matrix, highlighting their tendency to form a protective superficial oxide layer. This statement is also supported by the high concentration of oxygen in the same area, with values between a minimum of 4.63wt.% and maximum of 16.6wt.%O. Chemical composition analyses were also performed on areas where the Pb layer was detached (Fig. 8). The thickness of the layer affected by the action of molten lead was of maximum 8μm.

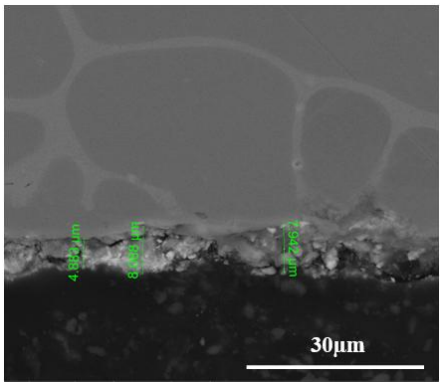

Fig. 8. Areas where the Pb layer was detached from the metallic sample [23].

In the superficial areas, eroded and partially attacked by molten lead, the oxide layer still contains a maximum of 19.12wt.%O, 8.57wt.% Zr and 6wt.%Y. These values confirm once again that complex oxide layers are formed on the alloy surface which protect the metallic matrix from the destructive action of molten lead. Another interesting aspect is given by the alloy behaviour during intense irradiation with radioactive isotopes of the Co^{-60} type [19-20].

Field et al. [26,27] have shown that in Fe-Cr-Al alloys subjected to high doses of neutron radiation, dislocation loops form which can develop micro-voids over time, or the embrittlement α′ phase may appear. In our paper, the presence of micro-voids was also identified near the surface of the analysed alloy (Fig. 9a). The

micro-voids show an obvious sphericity, and their marginal areas indicate deformation effects under internal pressure, with diameter between 5 and 25µm. Even in small amounts (1 to 2.5wt%), the microalloying elements Zr and Y form precipitates in the alloy matrix (Fig. 9b), which tend to agglomerate in the vicinity of the alloy surface. In contrast with the micro-void's aspect, intermetallic precipitates have a polyhedral configuration.

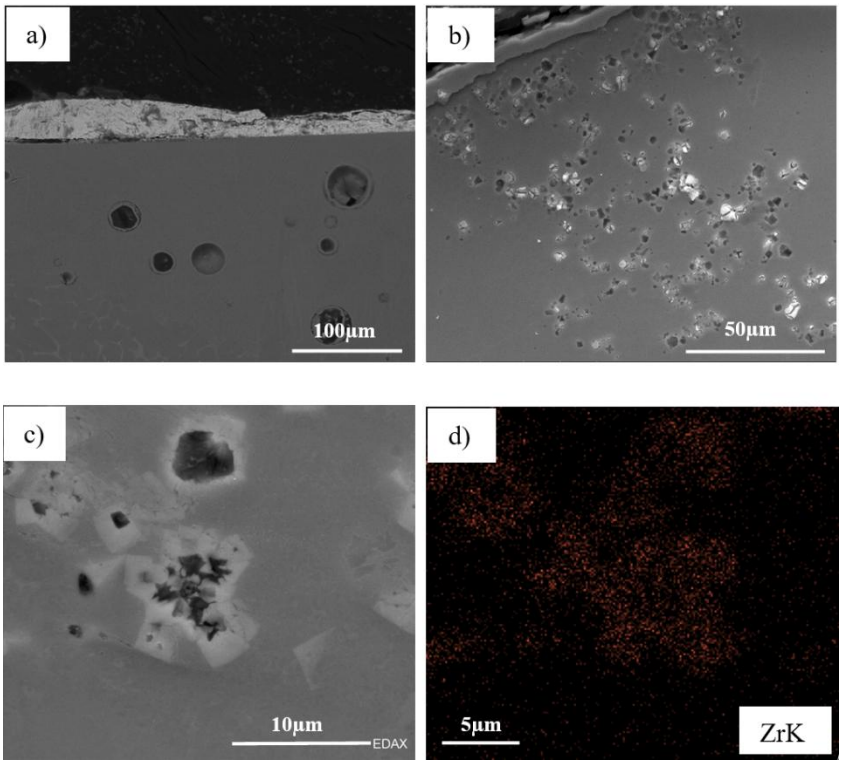

Fig. 9. Micro-voids formed as irradiation effect in laser processing area (a), inter-metallic precipitates accumulation near the alloy's surface (b), detail on Zr-rich precipitates (c) and EDS maps of Zr element (d).

Their interface with the matrix represents a "trap" on which the defects produced by irradiation are blocked (the formation and multiplication of dislocation loops, formation of voids in the ferrite crystal lattice, formation of embrittlement phases, appearance of oxide particles or films, etc.) [28]. The beneficial effect of laser processing can be seen in Fig. 10. Apart from the grain refinement, this area does not show massive irradiation defects, while in the no laser-processed metal matrix, networks of chained voids can be observed, which cause the material to deconsolidation and reduce its resistance to corrosion or erosion under the molten lead action. In Fig. 10b it can be seen how the working medium (liquid Pb) interacted with the metal, dissolving the oxide layer and infiltrating the grain

boundaries. The magnitude of this effect is, however, less important compared to the effects of irradiation on the base metal.

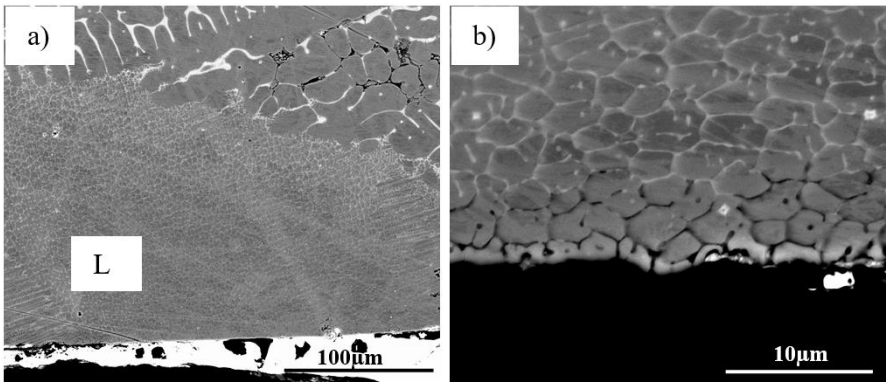

Fig. 10. Effects of irradiation in Fe16Cr8Al2.5Zr1.25Y alloy [8]. a) lead layer, laser processed zone (L) and base metal affected by irradiation; b) detail on laser processed edge zone.

3.2. Microhardness

Microhardness measurements were performed on sections taken transversely from the samples, aligned on their axis, along the diametrical axis of the section, with distances between indentations of at least 1000 microns. From the primary analysis of the experimental data, it was observed that on each sample there is a quasi-constancy of the microhardness values, which attests to an increased homogeneity of all samples made in RAV. For Fe-Cr-Al alloys microalloyed with Zr and Y, it is observed that there is a narrow range of microhardness values HV0.2 on the analyzed samples, ranging between 156 and 166 HV0.2, which is exclusively due to the influence of alloying elements in the composition of the metal alloy and the homogeneous arrangement of the constituents within the metal matrix. Also, a tendency for microhardness to increase with increasing Zr content in the alloy is observed, compared to the values recorded on the Fe16Cr8Al alloy without microalloying elements, which has microhardness values in the range of 148 – 154 HV0.2. The samples alloyed with Y show microhardness values in the range of 164 – 166HV0.2, which are within the normal limits of these alloys.

6. Conclusions

The addition of microalloying elements (Zr and Y) in the Fe-Cr-Al alloy led to the formation of intermetallic precipitates and a superficial layer of complex oxide, which allows increasing the resistance to the destructive action of molten lead. Superficial laser melting determined the advanced finishing of the microstructure but decreased resistance to the formation of defects generated by irradiation with radioactive isotopes.

The maximum diffusion distance of the elements coming from the working environment (Pb, O) was about 5µm from the surface of the Fe16Cr8Al2.5Zr1.25Y alloy. Lead shows the tendency to penetrate on the intergranular boundaries, favouring the slow dissolution of the areas unprotected by the complex oxide layer formed by the alloying elements.

Prolonged exposure to high doses of radiation can cause the appearance of internal defects such as micro-voids or dislocation networks, which, through coalescence, reduce the mechanical or corrosion resistance of the material.

The addition of the microalloying elements Zr and Y, separately or together, has the effect of slightly increasing the microhardness of the alloy, from the maximum value of 154HV0.2 to about 166HV0.2.

REFERENCES

[1] *G.S. Was, D. Petti, S. Ukai, S. Zinkle*, Materials for future nuclear energy systems, Journal of Nuclear Materials, Vol. **527,** art. 151837, 2019.

[2] *T. R Allen, D. C. Crawford,* Lead-Cooled Fast Reactor Systems and the Fuels and Materials Challenges, Science and Technology of Nuclear Installations, Vol. **3**, Art. 97486, 2007.

[3] *A. Jianu, A. Weisenburger, A. Heinzel, R. Fetzer, M. Delgiacco, W. An, G. Mueller, I. Voiculescu, V. Geantă,* Alumina scale formation on FeCrAl-alloys exposed to 400-600 °C in oxygen containing liquid lead (E11-P-1-12 (1961/1/1). European Congress on Advanced Materials and Process, EUROMAT, Montpellier, France, 2011.

[4] *H. Qu, L. Yin, M. Larsen, R.B. Rebak,* Distinctive Oxide Films Develop on the Surface of FeCrAl as the Environment Changes for Nuclear Fuel Cladding. Corros. Mater. Degrad. Vol. **5**, pp.109-123, 2024

[5] *M.F. Pillis, O.V. Correa, E.G. De Araújo, L.V. Ramanathan,* Oxidation Behavior of FeCr and FeCrY Alloys Coated with an Aluminium Based Paint. Materials Research, Vol. **11**, No. 3, pp.251-256, 2008.

[6] *V. Geanta , I. Voiculescu, R. Stefanoiu, A. Jianu, I. Milosan , E.M. Stanciu, A. Pascu, I.M. Vasile,* Titanium Influence on the Microstructure of FeCrAl Alloys Used for 4R Generation Nuclear Power Plants, Rev.Chim (Bucharest), Vol. **70**, Iss. 2, pp. 549-554, 2019.

[7] *V. Geanta, I. Voiculescu, R. Stefanoiu, A. Jianu,* Influence on chemical composition of FeCrAl alloys on the microhardness, Metalurgia International, Vol. **16**, Iss.5, pp.153-156, 2011.

[8] *H. Shi, R. Fetzer, A. Jianu, A. Weisenburger, A. Heinzel, F. Lang, G. Muller,* Influence of alloying elements (Cu, Ti, Nb) on the microstructure and corrosion behaviour of AlCrFeNi-based high entropy alloys exposed to oxygen-containing molten Pb, Corrosion Science, Vol. **190**, art. 109659, 2021.

[9] *I. Roy, H. Abouelella, R. Rajendran, A.S. Chikhalikar, M. Larsen, R. Umretiya, A. Hoffman, R. Rebak,* Effect of Al Concentration on Fe-17Cr Alloy during Steam Oxidation at 400 °C, Corros. Sci. Vol. **217**, 111135, 2023.

[10] *H. Shi, R. Fetzer, C. Tang, D. Vinga Szabo, S. Schlabach, A. Heinzel, A. Weisenburger, A. Jianu, G. Muller,* The influence of Y and Nb addition on the corrosion resistance of Fe-Cr-Al-Ni model alloys exposed to oxygen-containing molten Pb, Corrosion Science, Vol. **179**, art. 109152, 2021.

[11] *S.S. Raiman, K.G. Field, R.B. Rebak, Y. Yamamoto, K.A. Terrani,* Hydrothermal Corrosion of 2nd Generation FeCrAl Alloys for Accident Tolerant Fuel Cladding. J. Nucl. Mater. Vol. **536**, 152221, 2020.

[12] *B.A. Pint, Y. Zhang,* Performance of Al-rich content resistant coating for Fe based alloys. Materials and Corrosion, Vol. **62**, Iss. 6, pp. 549-560, 2010.

[13] *J. Wang, K. Yan, W. Huang, Z. Lu,* Mechanisms of Al_2O_3 and Cr_2O_3 formation during FeCrAl alloy Oxidation: A First-Principles study, Applied Surface Science, Vol. **644**, art.158782, 2024.

[14] *L.E. Geambazu, I. Voiculescu, C.A. Manea, R.V. Bololoi,* Economic Efficiency of High-Entropy Alloy Corrosion-Resistant Coatings Designed for Geothermal Turbine Blades: A Case Study, Applied Science-Basel, Vol.**12**, Iss. 14, Art. No. 7196, 2022.

[15] *V. Geantă, I. Voiculescu, D. Tenciu, L. Baschir, E.M. Stanciu, A. Pascu,* Effect of laser processing on the microstructure of the FeCrAl alloys, Journal of Optoelectronics and Advanced Materials, Vol. **22**, Iss. 7-8, pp. 411-418, 2020.

[16] *I. Csaki, R. Stefanoiu, V. Geanta, I. Voiculescu, M.G. Sohaciu, A. Soare, G. Popescu, S. Serghiuta,* Researches regarding the processing technique impact on the chemical composition, microstructure and hardness of AlCrFeNiCo high entropy alloy, REV. CHIM, Vol. **67**, Iss. 7, p. 1373-1377, 2016.

[17] *P. Kadolkar, N.B. Dahotre,* Variation of structure with input energy during laser surface engineering of ceramic coatings on aluminum alloys. Applied Surface Science, Vol. **199**, Iss. 1-4, pp. 222-233, 2002.

[18] *I. Voiculescu, V. Geanta, E.M. Stanciu, A.D. Jianu, C. Postolache, V. Fugaru,* Effect of Irradiation and Temperature on Microstructural Characteristic of FeCrAl Alloys, Acta Physica Polonica A, Vol.**134**, Iss.1, pp. 116-118, 2018.

[19] *A. Pascu, J.C. Mirza Rosca, E.M. Stanciu,* Laser cladding: From experimental research to industrial applications, Materials today: proceedings, Vol. **19**, p. 1059-1065, 2019.

[20] *G. Song, W. Wei, B. Liu, B. Shuai, G. Liu, K. Xue, Y. Chen,* Effects of the Laser Micromelting Process Parameters on the Preparation of Micron-Sized FeCrAl Coatings on Zr Alloy Surfaces. Materials (Basel) Vol. **29**, Iss.16 (23):7421, 2023.

[21] *L. Wang, L. Chai, S. Xu, S. Liu, S. Gan, L. Chen, X. He, T. Polcar, N. Daghbouj, B. Li*, Study on the corrosion behavior of laser surface remelted and laser cladding of ferritic/martensitic steels after exposure to lead-bismuth eutectic at 700 °C, Journal of Nuclear Materials,Vol. **590**,154888, Doi.org/10.1016/j.jnucmat.2023.154888, 2024.

[22] *Y. Chen, H. Zhu, P. Zhang, Z. Wang, M. Wang, G. Sha, H. Lin, J. Ma, Z. Zhang, Y. Song, et al.* An exceptionally strong, ductile and impurity-tolerant austenitic stainless steel prepared by laser additive manufacturing. Acta Mater. Vol. **250**:118868, 2023.

[23] Project No. PCCA 243/2014 Advanced Metallic Materials used for the New Generation of Nuclear Power Plant 4R – NUCLEARMAT.

[24] ISO/ASTM 51538:2009, Practice for use of the ethanol-chlorobenzene dosimetry system.

[25] *C.M. Petrie, K.G. Field,* Irradiation of Wrought FeCrAl Tubes in the High Flux Isotope Reactor, U.S. Department of Energy Advanced Fuels Campaign Linton Oak Ridge National Laboratory, NTRD: M3FT-17OR020203033, 2017.

[26] *K.G. Field, et al*. Radiation tolerance of neutron-irradiated model Fe-Cr-Al alloys, Journal of Nuclear Materials, Vol. **465**, pp. 746-755, 2015.

[27] *K.G. Field, et al.* Heterogeneous dislocation loop formation near grain boundaries in a neutron irradiated commercial FeCrAl alloy, Journal of Nuclear Materials, Vol. **483**, pp. 54-61, 2017.

[28] *Kefei Pei, Guang Ran, Yipeng Li, Ziqi Cao, Dewang Cui, Ruiqian Zhang, Gang Yang*, In-situ TEM study of loop evolution in FeCrAl alloy under Fe+ irradiation: Effects of temperatures, dislocations and precipitates, Nuclear Analysis, Vol. **1**, Iss. 1, art. 100001, 2022.